SDC Technical Note SDC-92172

Radiation Damage Studies for the SDC Electromagnetic Calorimeter

A. R. Fazely[a], R. Gunasingha, R. L. Imlay, E. S. Khosravi, Jit-Ning Lim[b], C. Lyndon, G. McMills, R. R. McNeil, W. J. Metcalf

Department of Physics and Astronomy
Louisiana State University,
Baton Rouge, LA 70803

J. C. Courtney and R. Tashakkori

Department of Nuclear Sciences
Louisiana State University,
Baton Rouge, LA 70803

B. J. Vegara

Department of Physics
Southern University,
Baton Rouge, LA 70813

January 19, 1992

Abstract

We report the results from a year long study at LSU aimed at radiation resistance and optical performance of scintillator tile with green wave shifter fiber readout. After careful investigation of several rad-hard plastic scintillators from Bicron and Kuraray, studies indicate that for a specific rad-hard Bicron scintillator, it is possible to build a tile/fiber EM calorimeter that can operate in the design luminosity of SSC. This calorimeter with excellent optical response would only have a light loss of about 5% after being exposed to 1 Mrad.

I. INTRODUCTION

The SDC experiment is designed to study proton-proton collisions at the SSC at energies and luminosities much higher than those of existing accelerators. The design specifications of the SSC of 40 TeV center-of-mass energy and initial luminosity of 10^{33} which could increase to 10^{34}, present a challenge to the existing widely used plastic scintillator based calorimeter technology. An important question is whether such a calorimeter can survive the high radiation environment of the SSC and maintain its optical integrity. The SDC physics goals spelled out in the LOI[1], require an overall resolution of $0.16/\sqrt{E}+0.01$. While the stochastic term is governed by the granularity of the calorimeter, the constant tern is dominated by the surface nonuniformity of the tile/fiber assembly. The crucial factor is that radiation damage should not increase the constant term above the goal of one percent.

This Technical Note describes the results of a lengthy search for a rad-hard scintillator and wave-length-shifter (WLS) fiber. It also contains the results of our optical performance studies and surface uniformity studies after radiation exposure which indicate that scintillator calorimetry will be able to meet the SDC goals.

II. EXPERIMENTAL ARRANGEMENT

In order to achieve a fairly quick, high-statistic scan for surface uniformity and radiation damage studies, we used a ^{106}Ru, β source. The end-point kinetic energy of the electrons for this

isotope is about 3.5 MeV. The initial strength of this source was 10 $\mu - Ci$. The source was attached to a motor arm which was programmed to move to different positions above either the test tile or the reference tile.

Our experimental setup, is shown in Fig. 1. A 16 cm by 25 cm by 1 cm thick scintillator was used for triggering on the β-rays. This counter was viewed by a 5.08 cm diameter Hammamatsu R878 photomultiplier tube (PMT) which was attached to the scintillator piece via an adiabatic plexiglass light-pipe. A curved, 0.25 cm thick, green WLS, Y7 light guide assembled under the trigger counter was viewed through a green wave-shifter "cookie" by an R878 PMT, as shown in Fig. 1. A 2.5 mm passive tile was mounted on the top of the trigger tile and under the test and the reference tiles. The light from the reference tile or the test tile could be read out by the curved WLS-light guide. The test tile alternatively could also be read out via optical fiber, as shown in Fig. 1. The reference tile was grooved for fiber readout via either a R878 PMT or a calibrated R201 Hammamatsu PMT. A large cosmic-ray veto counter was mounted under the scanning table in order to further reduce the number of cosmic ray events.

III. SCINTILLATOR TILES

During the latter part of 1990 and the fist half of 1991, we received several shipments of scintillator tiles from Bicron. These tiles were nominally 10 cm by 10 cm by 2.5 mm thick. Table I shows the nomenclature used by Bicron to identify these tiles. We also had in our possession a number SCSN-

38 Kuraray tiles which were used in the ZEUS calorimeter as well as some obtained from Ohio State University. Recently, a few SCSN-81 tiles were obtained from Florida State University.

All of the tiles received from Bicron were diamond-mill cut and no polishing was required. Some of the SCSN-38 tiles had to be cut from a bigger sheet of scintillator and the edges were polished. The batch of SCSN-38 tiles obtained from OSU were laser cut and required no polishing. The SCSN-81 tiles received from FSU had to be cut and polished. We did not observe significant difference between the differently treated edges as far light collection and light yield were concerned. Every tile was washed and wrapped tightly in aluminized mylar.

IV. OPTICAL YIELD MEASUREMENTS

The brightness of the tiles were studied with our setup. The ^{106}Ru source was programmed to scan a 5 by 5 array on the tile surface. At each point a pulse height (PH) distribution was recorded, usually for 10000 triggers. Table II shows the average PH for each tile. The normalization is with respect to the average PH of the reference tile measured at its center. Furthermore, SCSN-38 is taken to be the yard-stick with which the PH for all of the other tiles were compared. Fig. 2 shows a typical PH distribution for a tile in which WLS light-guide readout was used. A high statistics PH distribution plot is shown in Fig. 3. Note that in latter case the one photo-electron (pe) and the two-pe peaks are clearly visible. The PH spectrum for the trigger scintillator is shown in Fig. 4. A software PH cut accepted only events which deposited more than

1.4 MeV in the trigger counter. This restricted acceptance to the high energy end of the β-decay spectrum.

Our geometry and the β spectrum were input to a Monte Carlo (MC) calculation using EGS4. Fig. 5 shows the MC energy spectrum for the trigger counter. The simulation closely reproduced the experimental data. Comparison of the data and MC energy spectra provided a relation between ADC channels and the energy deposition in MeV. The MC plots for the electron beam spread from the source are shown in Figs. 6 for the test tile.

The MC also shows that the spectrum of energy deposition in the test counter the is relatively narrow and close to that of a minimum-ionizing particle for events satisfying the trigger requirements. Thus the spread in the real spectrum is predominantly due to the photostatistics and the spectrum shape can be used to determine the average number of photoelectrons.

V. FIBER READOUT

As shown in Fig. 1 a tile could also be read out using a green WLS fiber placed in a groove in the tile. SDC has decided to use this fiber readout technology.

Tiles were grooved using a ball endmill. The size of the endmill was 1.19 mm. The mill rotated at a frequency of 2000 RPM. The translational speed of the mill was 10 cm/min. This speed and frequency yielded the best groove quality. The light-yield and the surface uniformity depend on the groove pat-

tern used. Several groove path-configurations were examined. These configurations are illustrated in Figs. 7-11.

Fibers were cut to a length of about 1 meter and were embedded inside the grooves using optical grease. All fibers used were BCF-91A, and were 1 mm in diameter. The best path configuration was the rounded-square configuration shown in Fig. 11. The best surface light-yield uniformity is achieved when the groove is very near the edge of the tile (about 1 mm from the edge). Shown in Fig. 12 is LEGO plot of the PH of a fiber readout with the groove 1 mm from the edge. Fig. 13 shows a histogram of PH's from 361 positions on the tile surface. We note that this distribution is very narrow with a fwhm of less than 3.5%. The question of how much this nonuniformity affects the constant term in the EM calorimeter will be studied using EGS later.

The light yield with fiber readout usually was about half of that with the WLS light guide readout used, but comparable with what one could obtain with a WLS in a full scale calorimeter. We measured the absolute number of pe's for several fiber readout cases. The number of pe's per minimum ionizing particle for RH-4-1 was about 2.8 ± 0.2. This is comparable to the number of pe's per layer for existing calorimeters such as that of ZEUS. Our measurements were repeated by our colleagues at ANL and were reproduced within uncertainties.[2]

VI. RADIATION DAMAGE STUDIES

After an initial source scan of each type of plastic tile, sam-

ples of each kind were exposed to approximately 1 Mrad of γ radiation at the LSU Nuclear Science Center. The γ-ray source was an annular array of ^{60}Co rods and plate clad in stainless steel centered in a pit under 5.5 m of water. The half-life of ^{60}Co is 5.7 years and its total activity measured on July 30, 1986 was 3071 Ci. An exposure of 1 Mrad required about 7.5 hours.

The samples were placed in a small aluminum cylinder and lowered into the cobalt pit for irradiation. Most samples were exposed to radiation in an air atmosphere, however, some samples were also exposed in a N_2 atmosphere. The ambient temperature was measured to be $25.6C^o$ within the chamber. The radiation induced heating in the tiles was negligible.

The dose rate along the centerline in the empty air-filled chamber varies as shown in Fig.14. This axial variation was further reduced by γ scattering within the tiles.

In order to monitor the level of radiation exposure of each tile, a photo-sensitive radiation dosimeter was attached to each tile. For some tiles dosimeters were placed at all four corners as well as the middle of the tiles. The variation in the absorbed dose over the tile surface was less than 10%.

VII. RESULTS

After exposure each tile was examined for color change. Without exception all of the Bicron tile turned yellow, although the degree of yellowness varied significantly from tile to

tile. The only tiles which consistently showed no color change were the SCSN-38 tiles. SCSN-81 also showed color change, however, not as dramatic as some of the Bicron tiles. These observations are tabulated in Table III.

Within an hour of removal from the ^{60}Co pit, each tile was rescanned for PH response. The scans thereafter continued for some period of time (usually 10 days) in order to obtain a recovery plot for irradiated sample tiles. A typical recovery curve is shown in Fig. 15. The striking feature of the plot is a two-component recovery curve, a fast component (a day or two) and a slow component. This is true for all of the Bicron tiles without exception. We also noted that the PH responses just after irradiation seem to be correlated with the change in color and the degree of yellowness, that is the yellower the tile the less the PH.

The Kuraray tiles responded very differently to radiation. The SCSN-38 tiles which are also being used for the ZEUS calorimeter were found to be the most rad-hard. The SCSN-81 tiles, received from FSU did not seem to be as rad-hard as the SCSN-38 tiles. There was some yellowness just after radiation exposure and some light loss, however, not as much as Bicron tiles. Fig. 16 and 17 show the recovery plots for samples of SCSN-38 tile and the SCSN-81 tile, respectively. Studies by the ZEUS collaboration[3] of the SCSN-38 show a 5% drop in the light yield for 1 Mrad. Our studies indicate a 15% light loss for the same scintillator. It would be desirable to study the variation of radiation hardness for tiles which are of the same type but produced at different times.

We also received small 5 cm diameter, 3 mm thick disks from Bicron. These disks were very rad hard and recovered fully. Fig. 18 shows the recovery for one of these disks. This recovery plot was extracted when a WLS plate readout was used. Fig. 19 shows a recovery plot in which a fiber readout was employed. The fiber was wrapped twice around the circumference of the disk. This procedure was reproducible to about 5%. It is noteworthy that although the chemical formulae of the tiles and the disks are very similar, the engineering process are very different. We therefore, believe that processing techniques in producing tiles may have a negative impact on the radiation hardness of the tiles. Most of the damage seem to occur on the tile surface. Note that none of the tiles we have tested either from Bicron or Kuraray have fully recovered. This is indeed of concern to us and developing a process for manufacturing rad-hard tiles is of essential importance to the success of scintillator-based calorimeter technology.

We extracted some information for optical properties of the tiles as a result of our 5 by 5 scans. There is a marked PH enhancement near the light guide. This is probably because of a two component fluor and the optics of the scintillator-light pipe assembly.[4] As shown in Fig. 20, the attenuation properties of the scintillator tiles do not change as a result of radiation exposure. Several tile fiber assemblies were exposed to radiation as a whole. Although the recovery was only to about 70% of the original level, the surface uniformity did not deteriorate as a result of radiation. This together with the attenuation length nonsensitivity to radiation were very encouraging because it

indicates that the constant term in the resolution will not be affected significantly as the calorimeter is exposed to radiation. These results are preliminary and should be investigated further.

Radiation damage was also studied as a function of dose and dose rate. Samples of Bicron and Kuraray tiles were exposed to 0.20, 0.30, 0.50, 0.75 and 1.0 Mrad (Fig. 21). It seems that the threshold for which permanent damage occurs is between 0.30 and 0.50 Mrad. The radiation exposure were applied much more quickly than would be the case at the SSC. With the standard setup, tiles received one Mrad in about 8 hours. As a check on possible dose-rate dependence some samples were exposed to 1 Mrad in a 56 hour period. No noticeable difference in radiation damage was observed at these two dose rates. Measurements at slower rates, for example, a few hundred rads per hour should be performed in order to understand long-term effects of damage in scintillators due to radiation exposure. There were also a set of measurements in N_2 atmosphere. For the types of scintillators tested, we did not observe any difference between air and N_2 environment.

Green WLS fibers were also exposed to radiation. We found BCF-91A to be very rad hard. Fig. 22 shows the recovery of the BCF-91A, WLS fiber. We also had samples BCF-91A fibers with defective cladding which showed significant radiation damage.

VIII. CONCLUSIONS

In conclusion, we believe that our preliminary studies show that it is possible to build a calorimeter with scintillator tile/fiber readout which can function in the SSC environment. These studies imply that the chemistry of rad hardness is probably understood by the manufacturers, however, the processing techniques and surface treatment of tiles have to be looked at more closely. It is important to continue these studies to understand long-term radiation damage behavior, aging and attenuation properties of both tiles and WLS fibers.

ACKNOWLEDGEMENTS

We are very grateful to staff of the LSU physics department machine shop, Leo Jordan, Ivan Shuff and Allen Young for the great job they did for us. We are also thankful to Dr. Charles Hurlbut of Bicron, Drs. James Proudfoot and David Underwood of ANL for their invaluable support.

REFERENCES

(a) Present address: Department of Physics, Southern University, Baton Rouge, LA 70813.
(b) Present address: Department of Physics, Pennsylvania State University, College Park, PA 40823.

[1] "Letter of Intent" by the Solenoidal Detector Collaboration, Note SDC-90-00151 (30 November 1990).
[2] D. Underwood, private communication.
[3] "The ZEUS Detector, Status Report 1987", ZEUS Collaboration, PRC87-02 (September 1987)
[4] B. G. Bylsma, et al., "Optical Readout Components for the ZEUS Barrel Calorimeter", Submitted to NIM.

FIGURE CAPTIONS

1. Perspective view of the test setup.

2. A typical PH spectrum for a tile with WLS light-guide read out.

3. A high statistics PH spectrum for a tile with WLS light-guide read out.

4. PH spectrum for the trigger counter.

5. MC simulated PH spectrum for the trigger counter.

6. MC simulated beam spread from the source in the test tile.

7-11. Groove-path configurations which were studied for light yield and surface uniformity.

12. Tile surface uniformity scan for fiber read out. The groove is right on the edge of the tile.

13. Position vs. PH histogram. All PH.s are normalized to the middle PH value.

14. Axial variation of the ^{60}Co.

15. Recovery plot for a typical BICRON tile after 1 Mrad exposure.

16. Recovery sample plot for one of the SCSN-38. Kuraray tiles after 1 Mrad exposure.

17. Recovery sample plot for one of the SCSN-81. Kuraray tiles after 1 Mrad exposure.

18. Recovery plot for one of the BICRON disks read with WLS light-guide after 1 Mrad.

19. Recovery plot for one of the BICRON disks read with WLS fiber after 1 Mrad exposure.

20. Recovery plots for BICRON tiles as a function of position along the tile before and after radiation exposure.

21. Recovery plots for BICRON tiles as a function of the total dose .

22. Recovery BICRON green WLS fiber (BCF-91A) after 1 Mrad exposure.

TABLE I

Scintillator Tiles and Disks Nomenclatures

Vendor	*Book No.*	*Chemical No.*	*Source*
KURARAY	*NONE*	$SCSN-38$	LSU/OSU
KURARAY	*NONE*	$SCSN-81$	FSU
BICRON	$HP-BC499-05$	$RH4/NA$	BICRON
BICRON	$HP-BC499-05$	$RH4/NA^*$	BICRON
BICRON	$HP-BC499-15$	$RH4/38$	BICRON
BICRON	$HP-BC499-17$	$RH4/A-36$	BICRON
BICRON	*NONE*	$RH1-M$	BICRON
BICRON	*NONE*	$RH1-1$	BICRON
BICRON	*NONE*	$RH1-2$	BICRON
BICRON	*NONE*	$RH1-3$	BICRON
BICRON	*NONE*	$RH1-4$	BICRON
BICRON	*NONE*	$RH1-5$	BICRON
BICRON	*NONE*	$RH1-6$	BICRON
BICRON	*NONE*	$RH4-1$	BICRON
BICRON	*NONE*	$RH4-2$	BICRON
BICRON	*NONE*	$RH4-3$	BICRON
BICRON	*NONE*	$RH4-4$	BICRON
BICRON	*NONE*	$RH4-6$	BICRON
BICRON	*NONE*	$RH4-7$	BICRON

TABLE I (continued)

Scintillator Tiles and Disks Nomenclatures

Vendor	*Book No.*	*Chemical No.*	*Source*
BICRON	*NONE*	$SW^{-}M - 10 - 82 : 1$	BICRON
BICRON	*NONE*	$SW^{-}M - 10 - 82 : 2$	BICRON
BICRON	*NONE*	$SW^{-}M - 10 - 82 : 3$	BICRON
BICRON	*NONE*	$W^{-}FH6 - 89 - 1$	BICRON
BICRON	*NONE*	$W^{-}FH6 - 89 - 2$	BICRON
BICRON	*NONE*	$W^{-}FH6 - 89 - 3$	BICRON
BICRON	*NONE*	$W^{-}FH6 - 89 - 4$	BICRON
BICRON	*NONE*	$W^{-}FH6 - 89 - 5$	BICRON
BICRON	*NONE*	$W^{-}FH6 - 89 - 6$	BICRON

TABLE II

Scintillator Tiles Relative PH (SCSN-38 = 1.0)

Vendor	*Chemical No.*	*Relative PH*
KURARAY	$SCSN-38$	1.00
KURARAY	$SCSN-81$	0.85
BICRON	$RH4/NA$	0.50
BICRON	$RH4/NA^*$	1.05
BICRON	$RH4/38$	1.50
BICRON	$RH4/A-36$	1.08
BICRON	$RH1-M$	0.80
BICRON	$RH1-1$	1.49
BICRON	$RH1-2$	1.28
BICRON	$RH1-3$	1.02
BICRON	$RH1-4$	0.86
BICRON	$RH1-5$	1.12
BICRON	$RH1-6$	0.97
BICRON	$RH4-1$	1.20
BICRON	$RH4-2$	1.26
BICRON	$RH4-3$	1.29
BICRON	$RH4-4$	1.08
BICRON	$RH4-6$	1.16
BICRON	$RH4-7$	1.02

TABLE II (continued)

Scintillator Tiles Relative PH

Vendor	*Chemical No.*	*Relative PH*
BICRON	$WFH6-89-1$	1.27
BICRON	$WFH6-89-2$	1.31
BICRON	$WFH6-89-3$	1.28
BICRON	$WFH6-89-4$	1.15
BICRON	$WFH6-89-5$	1.86
BICRON	$WFH6-89-6$	1.39

TABLE III

Visual Observations of Scintillator Radiation Damage

Tile	*Dose (Mrad)*	*Color*	*Source*
$RH4/NA$	1.00	yellow	BICRON
$RH4/NA^*$	1.00	yellow	BICRON
$RH4/38$	1.00	yellow	BICRON
$RH4/A-36$	1.00	yellow	BICRON
$RH1-M$	1.00	yellow	BICRON
$RH1-1$	1.00	orange	BICRON
$RH1-2$	1.00	orange	BICRON
$RH1-3$	1.00	yellow	BICRON
$RH1-4$	1.00	orange	BICRON
$RH1-5$	1.00	yellow	BICRON
$RH1-6$	1.00	yellow	BICRON
$RH4-1$	1.00	yellow	BICRON
$RH4-2$	1.00	yellow	BICRON
$RH4-3$	1.00	yellow	BICRON
$RH4-4$	1.00	yellow	BICRON
$RH4-6$	1.00	yellow	BICRON
$RH4-7$	1.00	yellow	BICRON
$SCSN-38$	1.00	no change	KURARAY
$SCSN-81$	1.00	slightly yellow	KURARAY

TABLE III (continued)

Visual Observations of Scintillator Radiation Damage

Vendor	*Book No.*	*Chemical No.*	*Source*
$SWM - 10 - 82 : 1$	1.00	slightly yellow	BICRON
$SWM - 10 - 82 : 2$	1.00	slightly yellow	BICRON
$SWM - 10 - 82 : 3$	1.00	slightly yellow	BICRON
$WFH6 - 89 - 1$	1.00	slightly yellow	BICRON
$WFH6 - 89 - 2$	1.00	slightly yellow	BICRON
$WFH6 - 89 - 3$	1.00	slightly yellow	BICRON
$WFH6 - 89 - 4$	1.00	slightly yellow	BICRON
$WFH6 - 89 - 5$	1.00	slightly yellow	BICRON
$WFH6 - 89 - 6$	1.00	slightly yellow	BICRON

L ILE/FIBER SCANNING SETUP

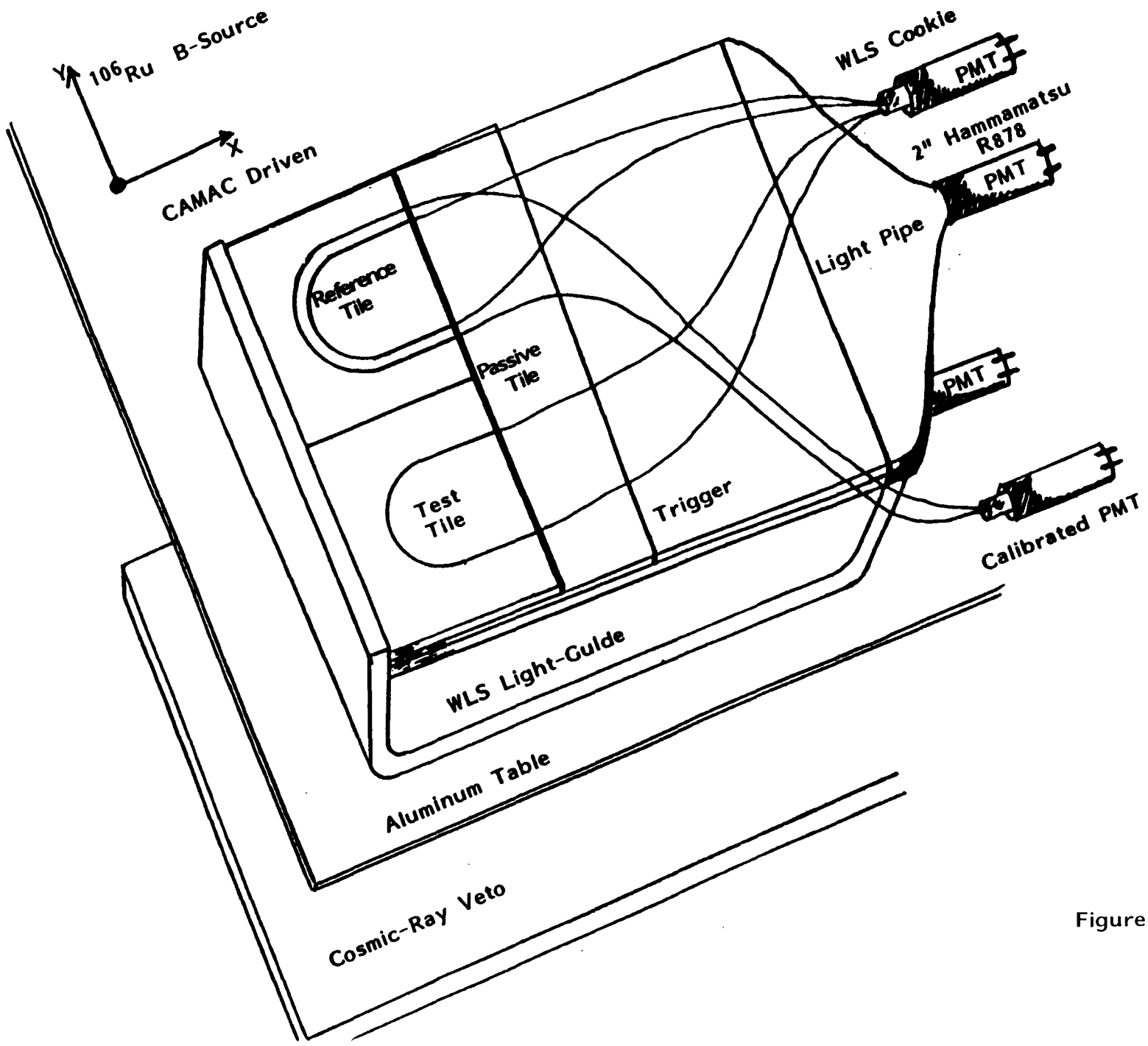

Figure 1

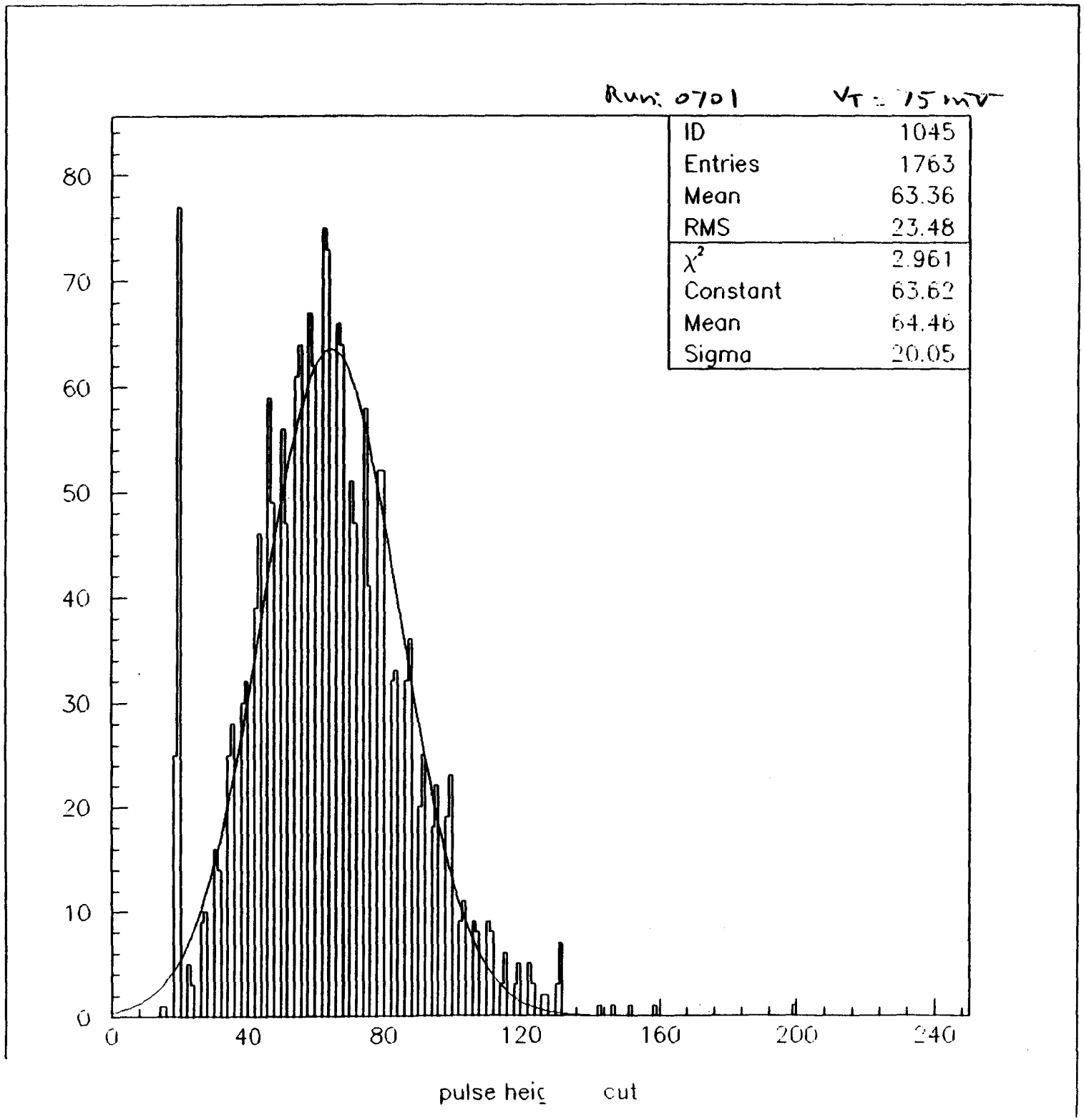
Run: 0701
V_T = 15 mV
ID 1045
Entries 1763
Mean 63.36
RMS 23.48
χ^2 2.961
Constant 63.62
Mean 64.46
Sigma 20.05
0
10
20
30
40
50
60
70
80
0
40
80
120
160
200
240
pulse heig cut

Figure 2

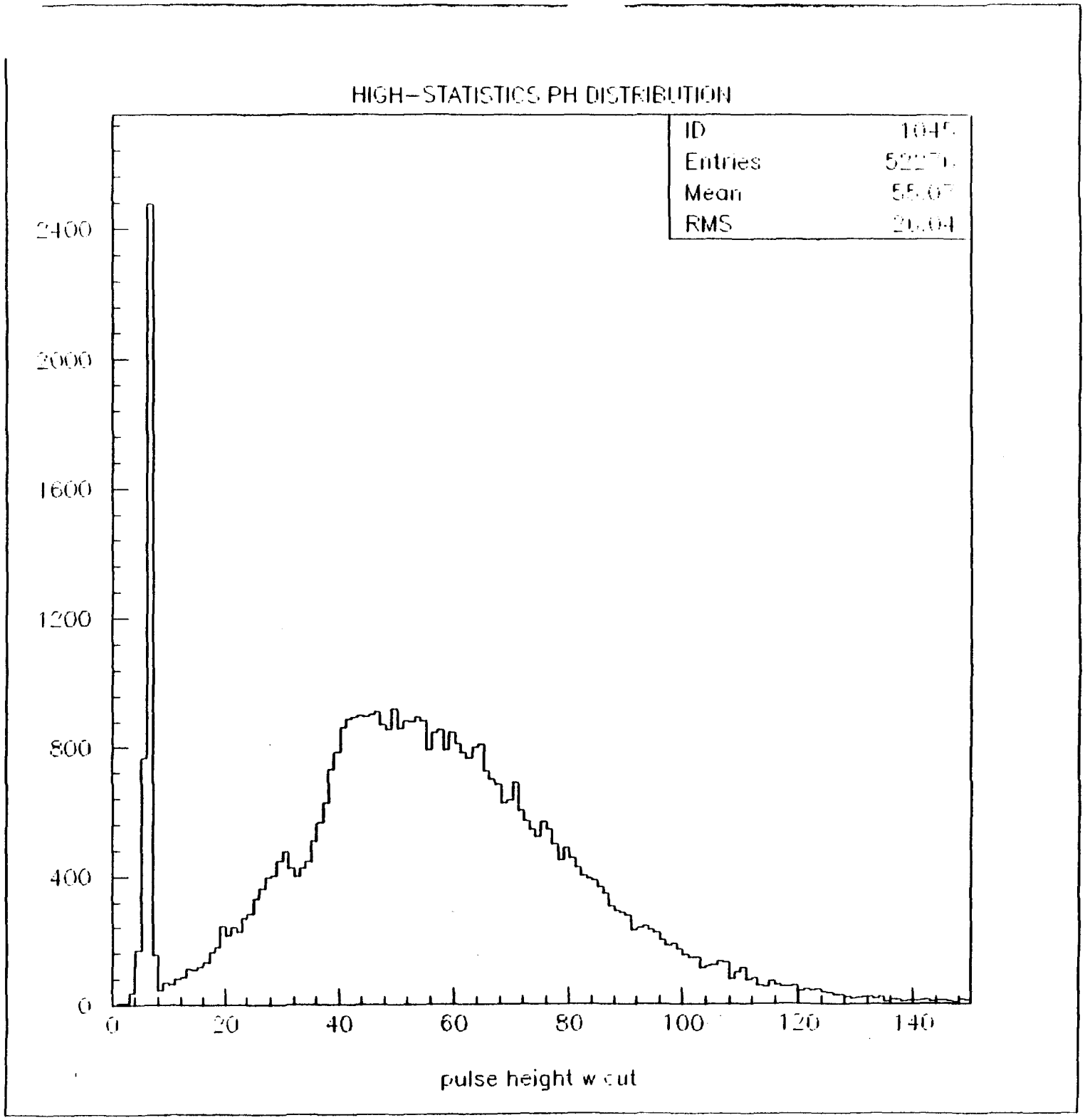
HIGH-STATISTICS PH DISTRIBUTION
ID
Entries
Mean
RMS
2400
2000
1600
1200
800
400
0
0
20
40
60
80
100
120
140
pulse height w cut

Figure 3

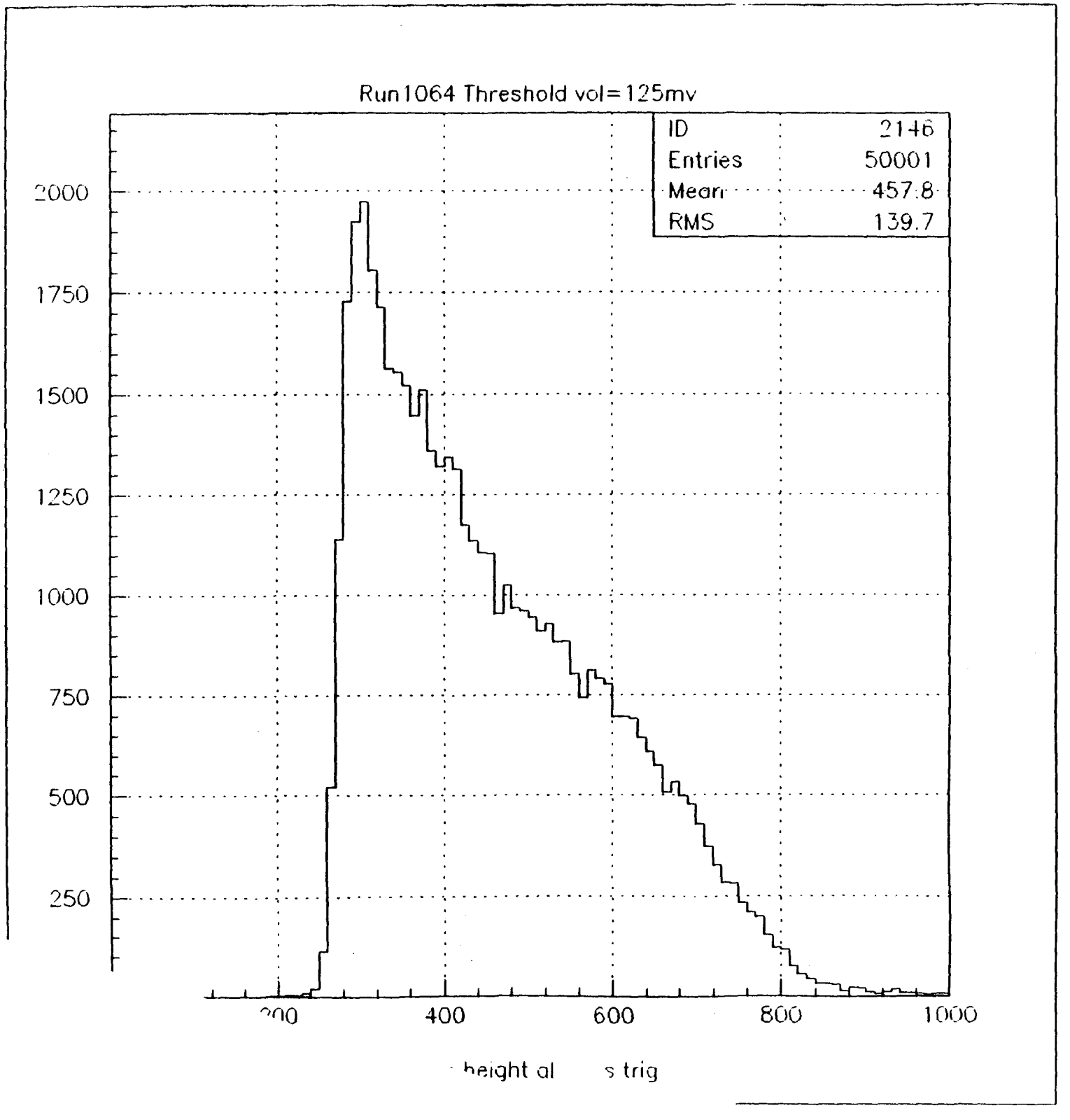
Run1064 Threshold vol=125mv
ID 2146
Entries 50001
Mean 457.8
RMS 139.7
2000
1750
1500
1250
1000
750
500
250
200
400
600
800
1000
height al s trig

Figure 4

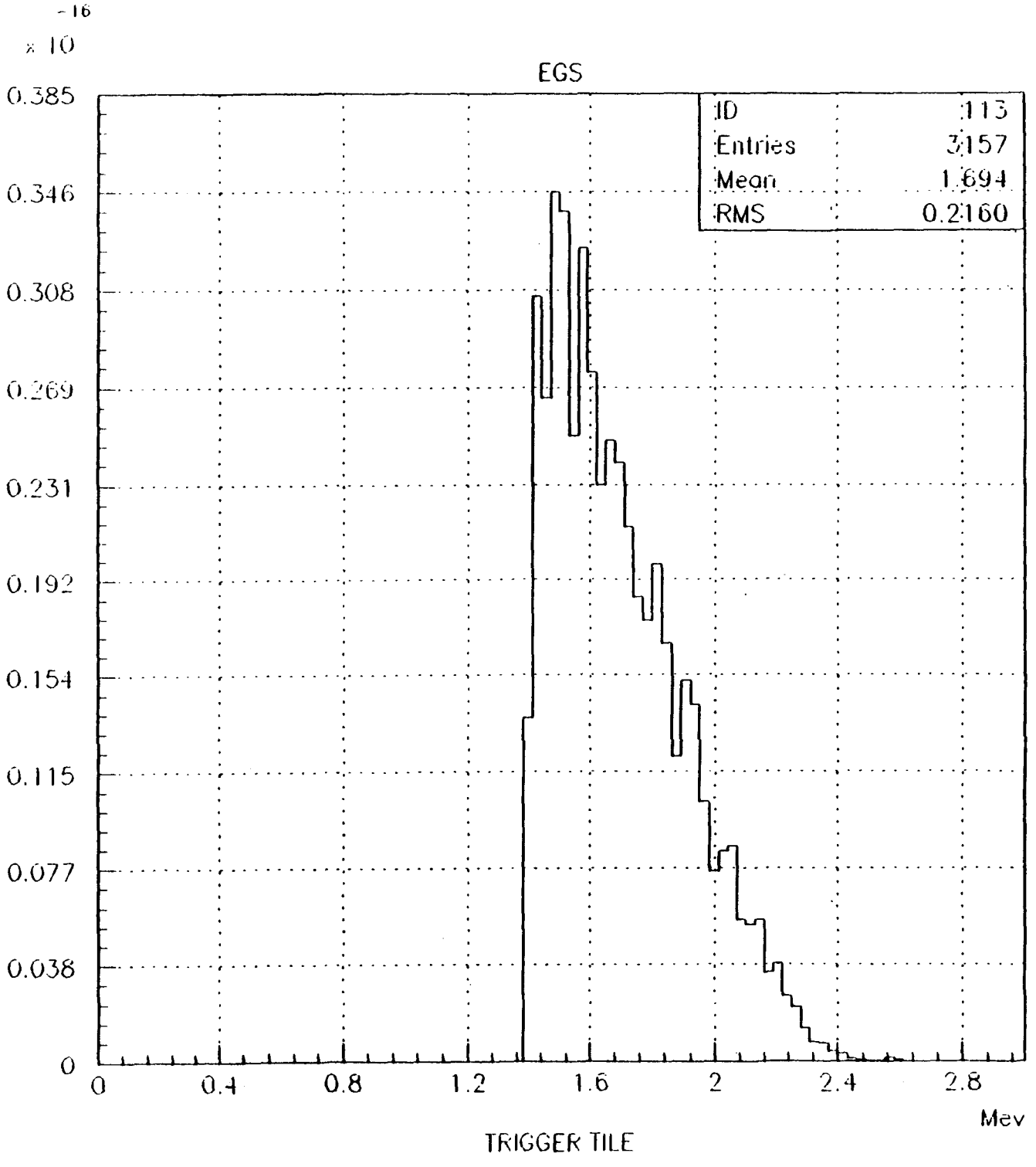
EGS
ID 113
Entries 3157
Mean 1.694
RMS 0.2160
0.385
0.346
0.308
0.269
0.231
0.192
0.154
0.115
0.077
0.038
0
0
0.4
0.8
1.2
1.6
2
2.4
2.8
Mev
TRIGGER TILE

Figure 5

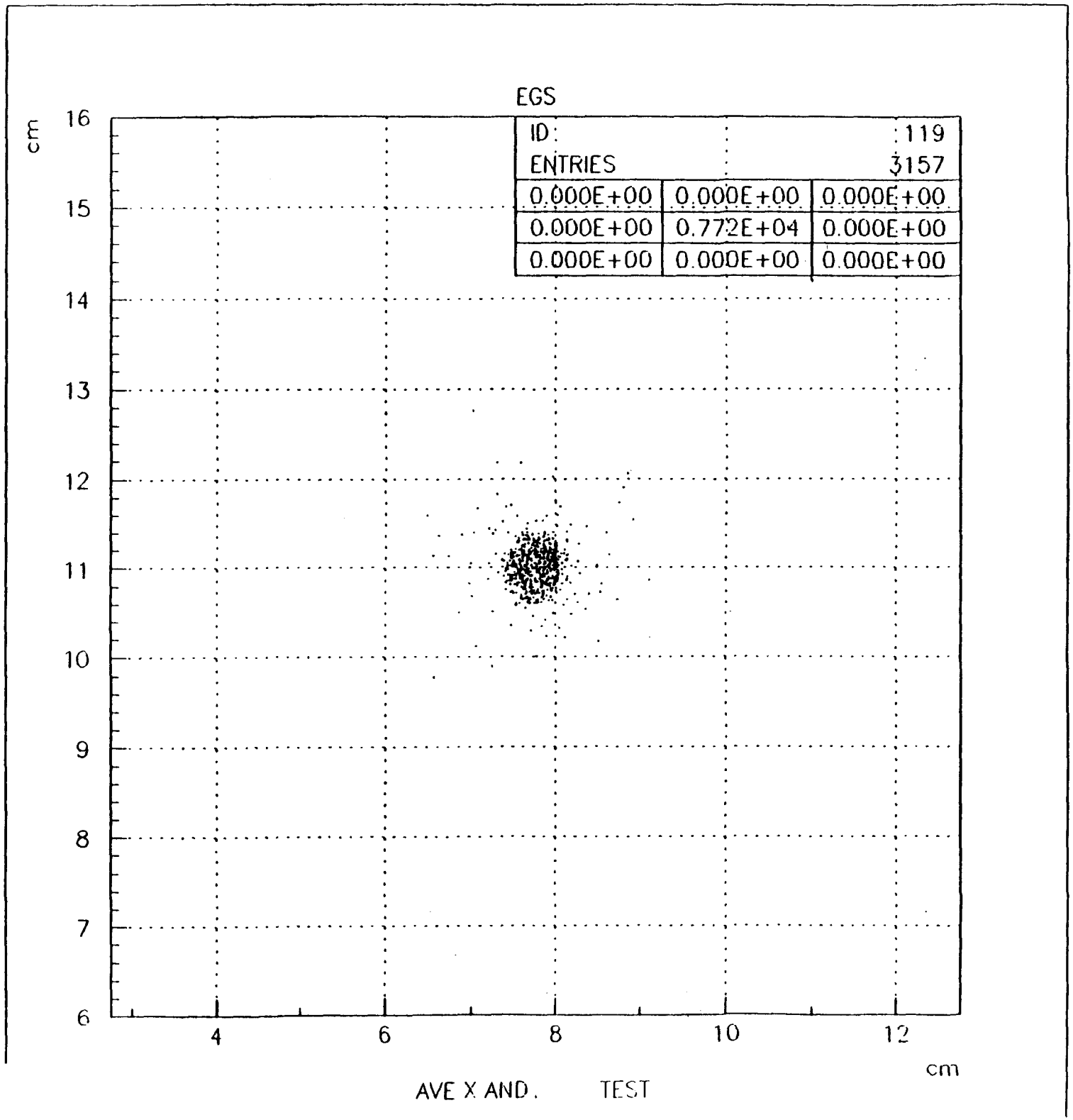
EGS
ID: 119
ENTRIES 3157
0.000E+00 0.000E+00 0.000E+00
0.000E+00 0.772E+04 0.000E+00
0.000E+00 0.000E+00 0.000E+00
cm
16
15
14
13
12
11
10
9
8
7
6
4
6
8
10
12
cm
AVE X AND . TEST

Figure 6

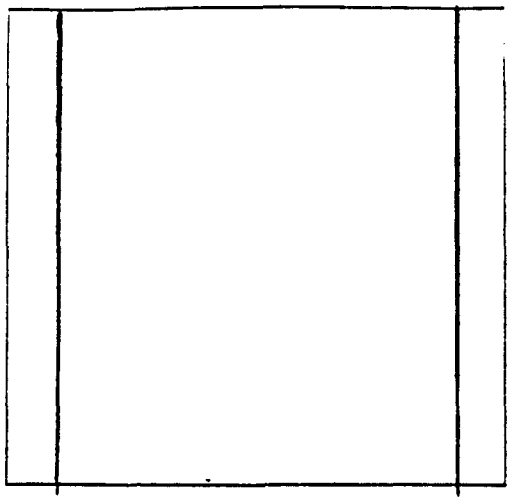

Figure 7

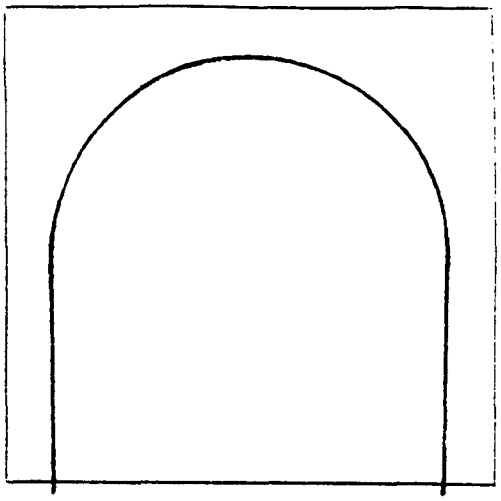

Figure 8

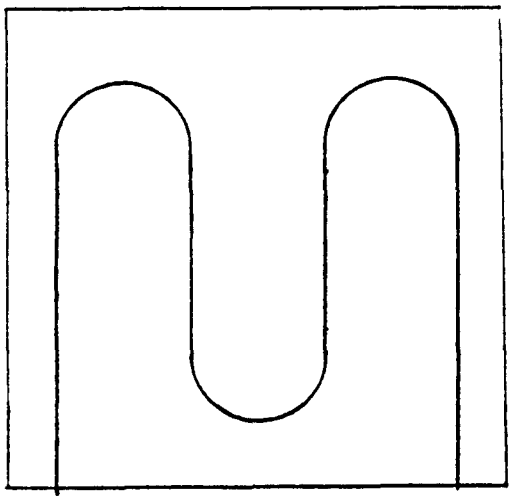

Figure 9

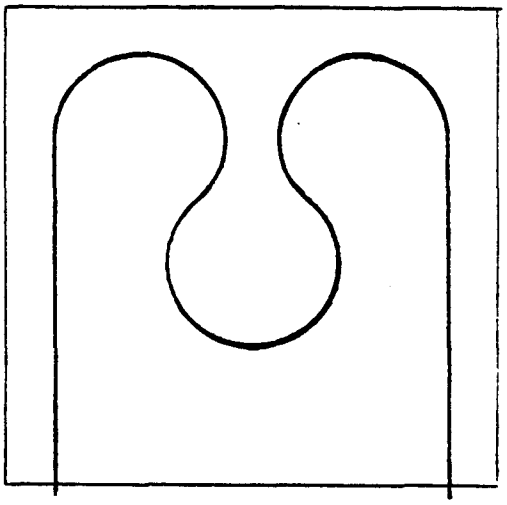

Figure 10

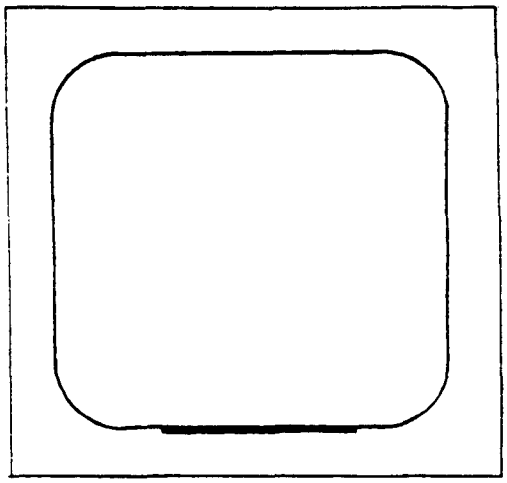

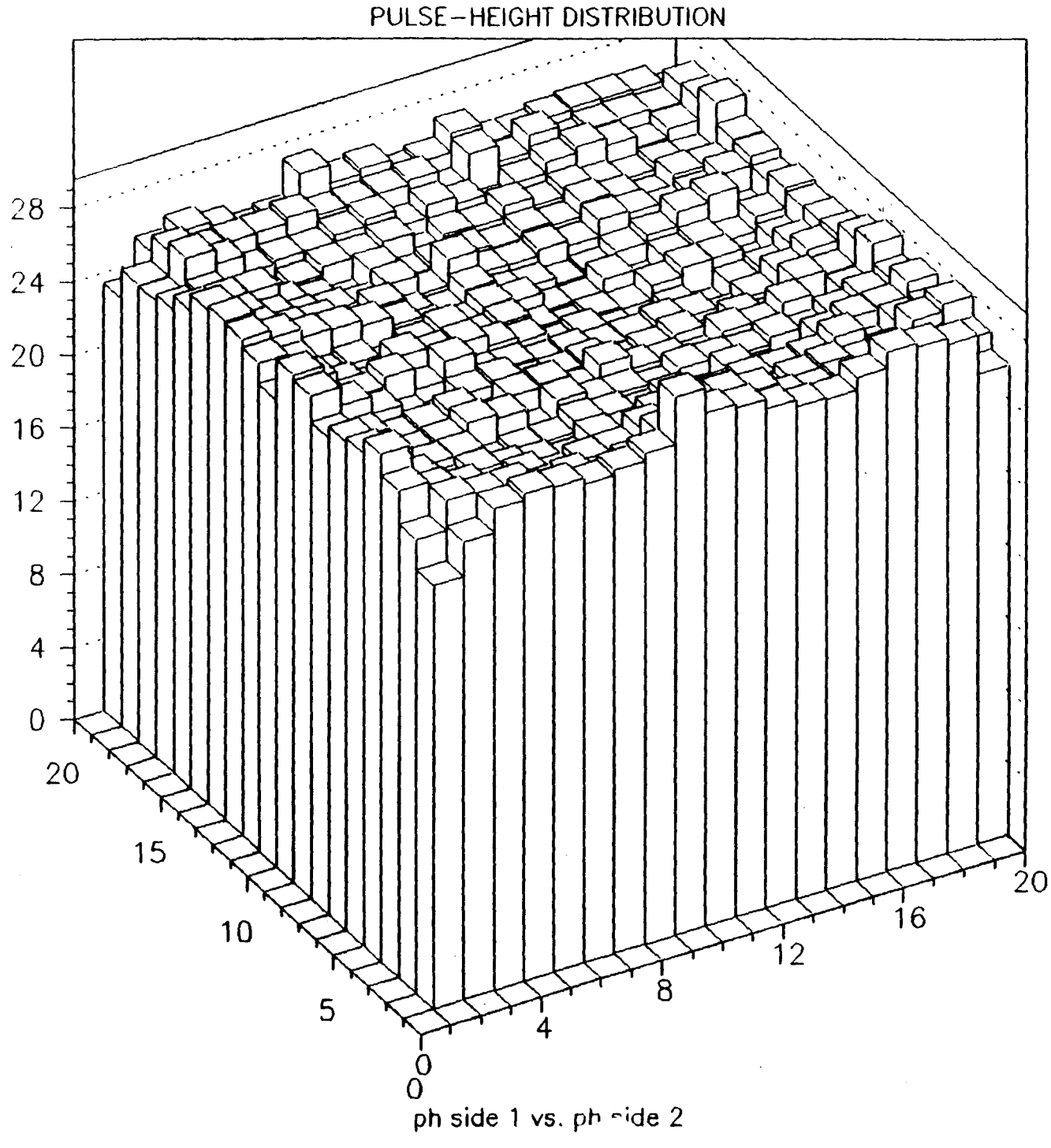
PULSE-HEIGHT DISTRIBUTION
28
24
20
16
12
8
4
0
20
15
10
5
0
0
4
8
12
16
20
ph side 1 vs. ph side 2

Figure 12

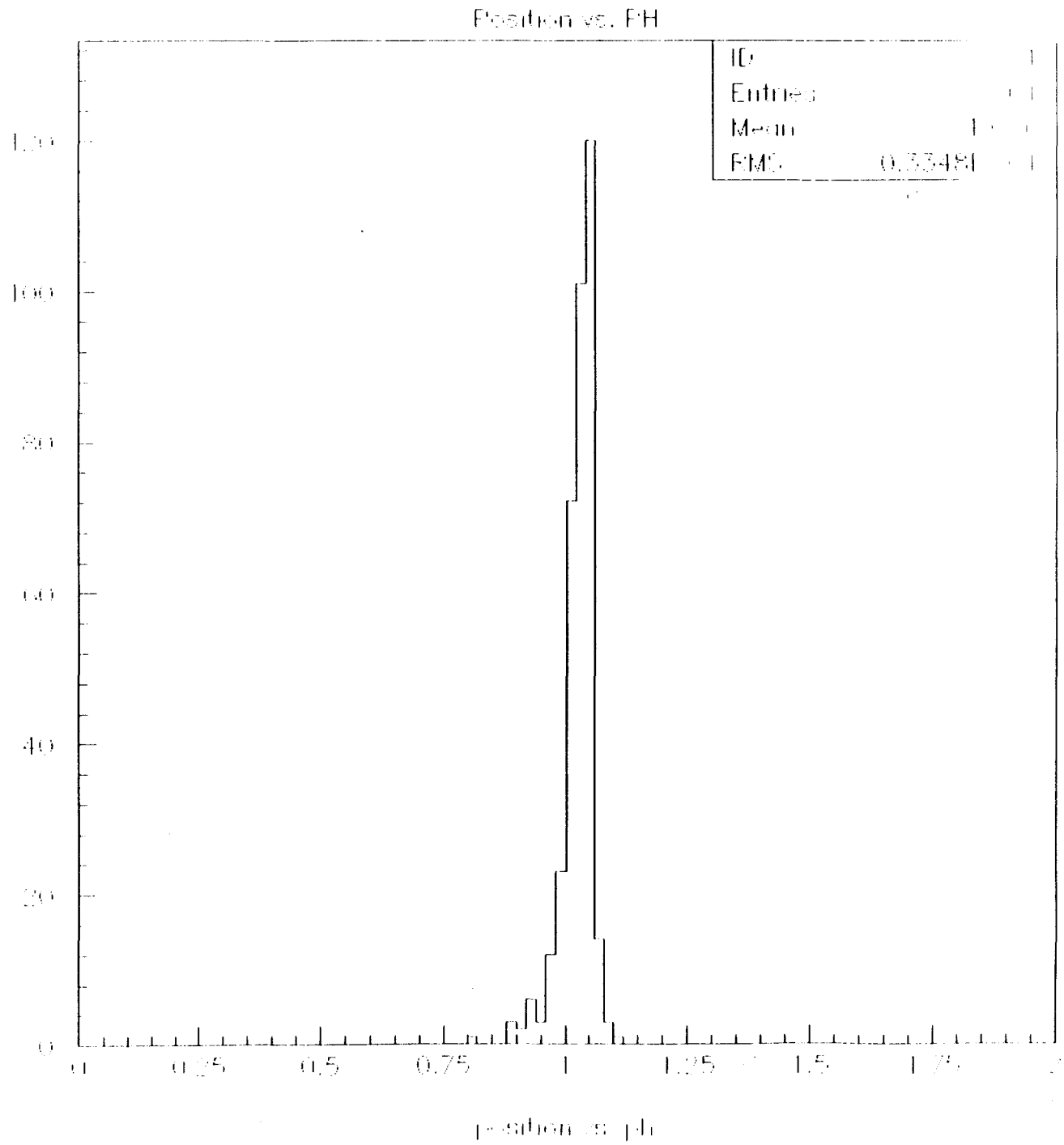

Figure 13

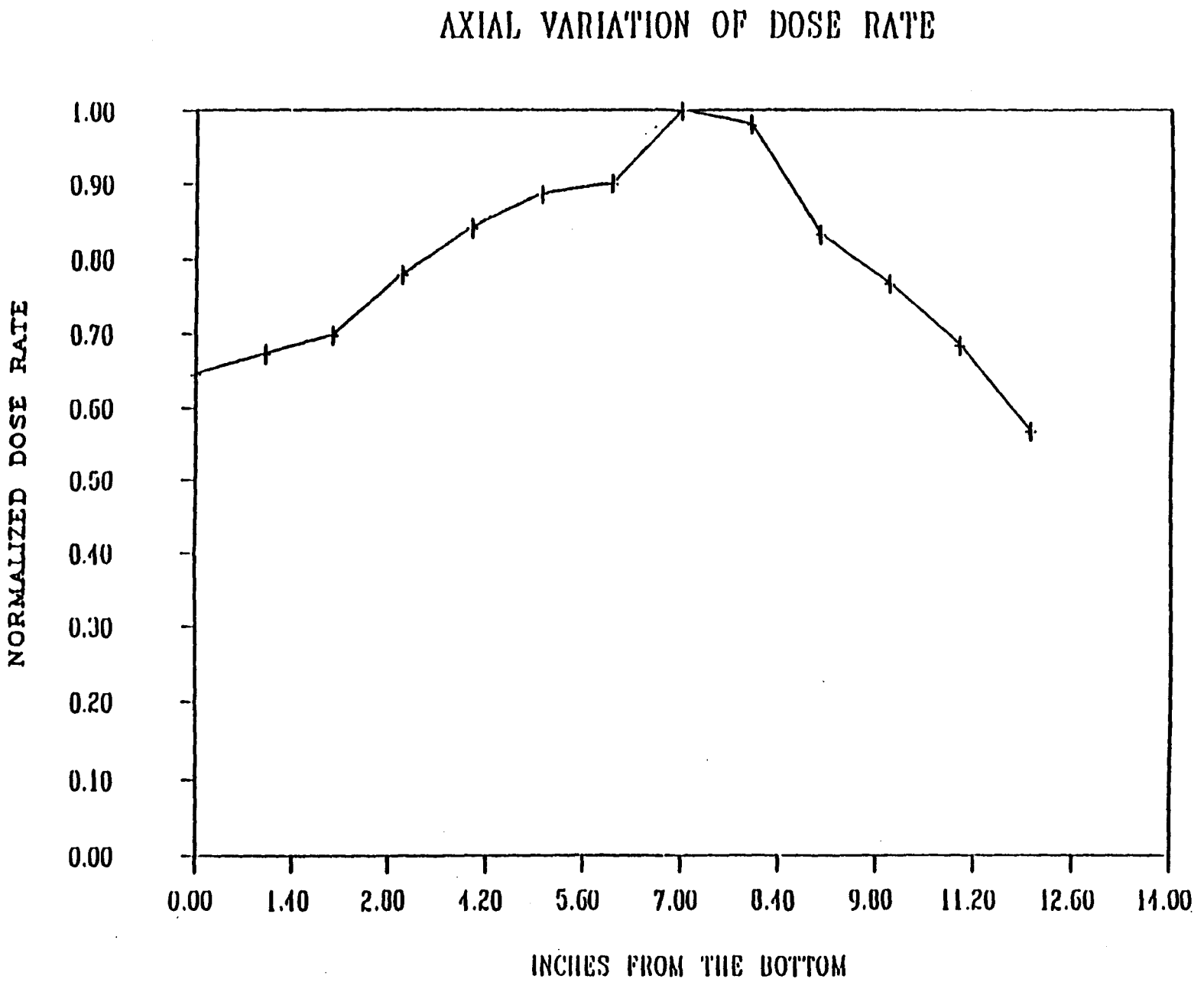
AXIAL VARIATION OF DOSE RATE
NORMALIZED DOSE RATE
1.00
0.90
0.80
0.70
0.60
0.50
0.40
0.30
0.20
0.10
0.00
0.00
1.40
2.80
4.20
5.60
7.00
8.40
9.80
11.20
12.60
14.00
INCHES FROM THE BOTTOM

Figure 14

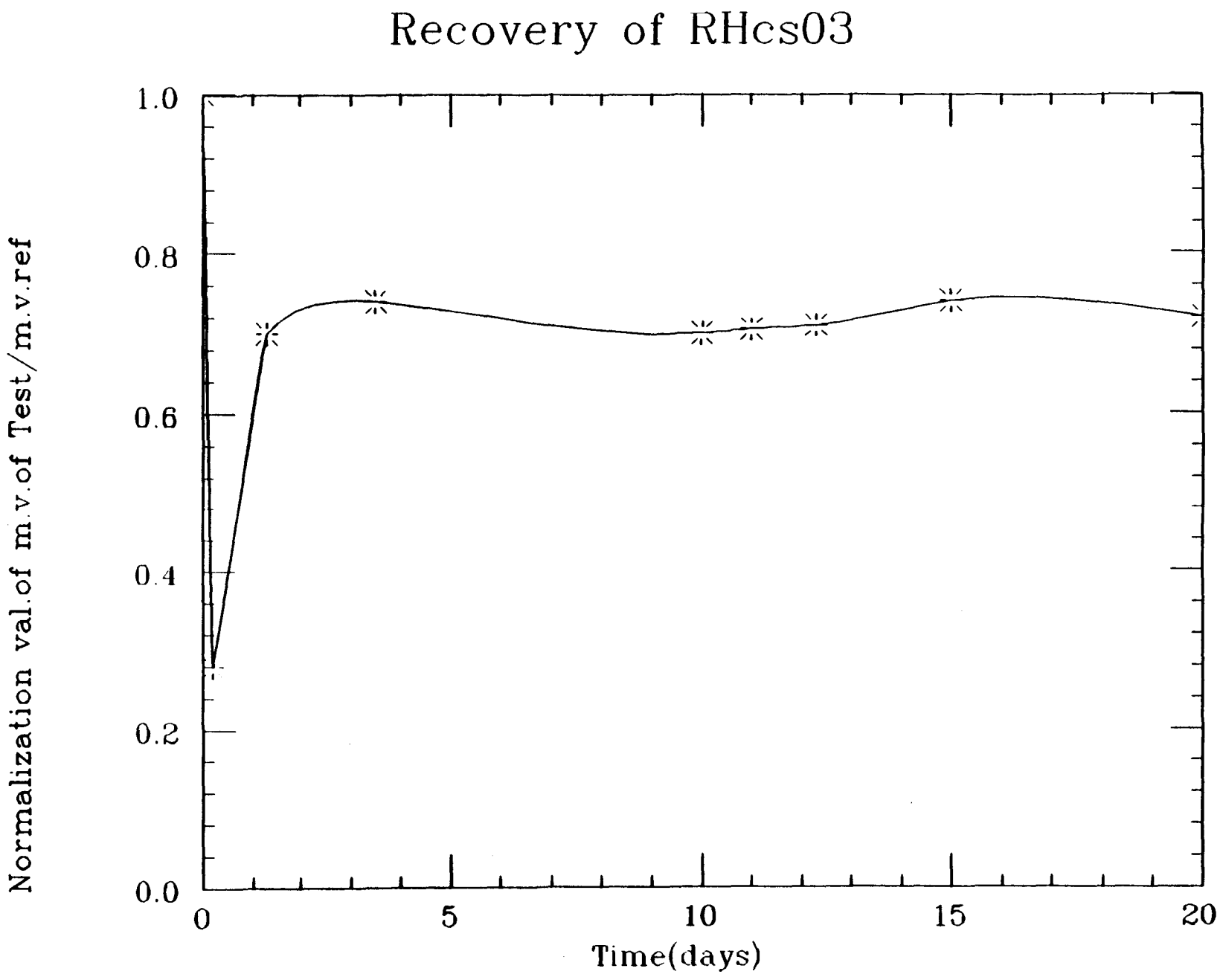
Recovery of RHcs03
Normalization val.of m.v.of Test/m.v.ref
1.0
0.8
0.6
0.4
0.2
0.0
0
5
10
15
20
Time(days)

Figure 15

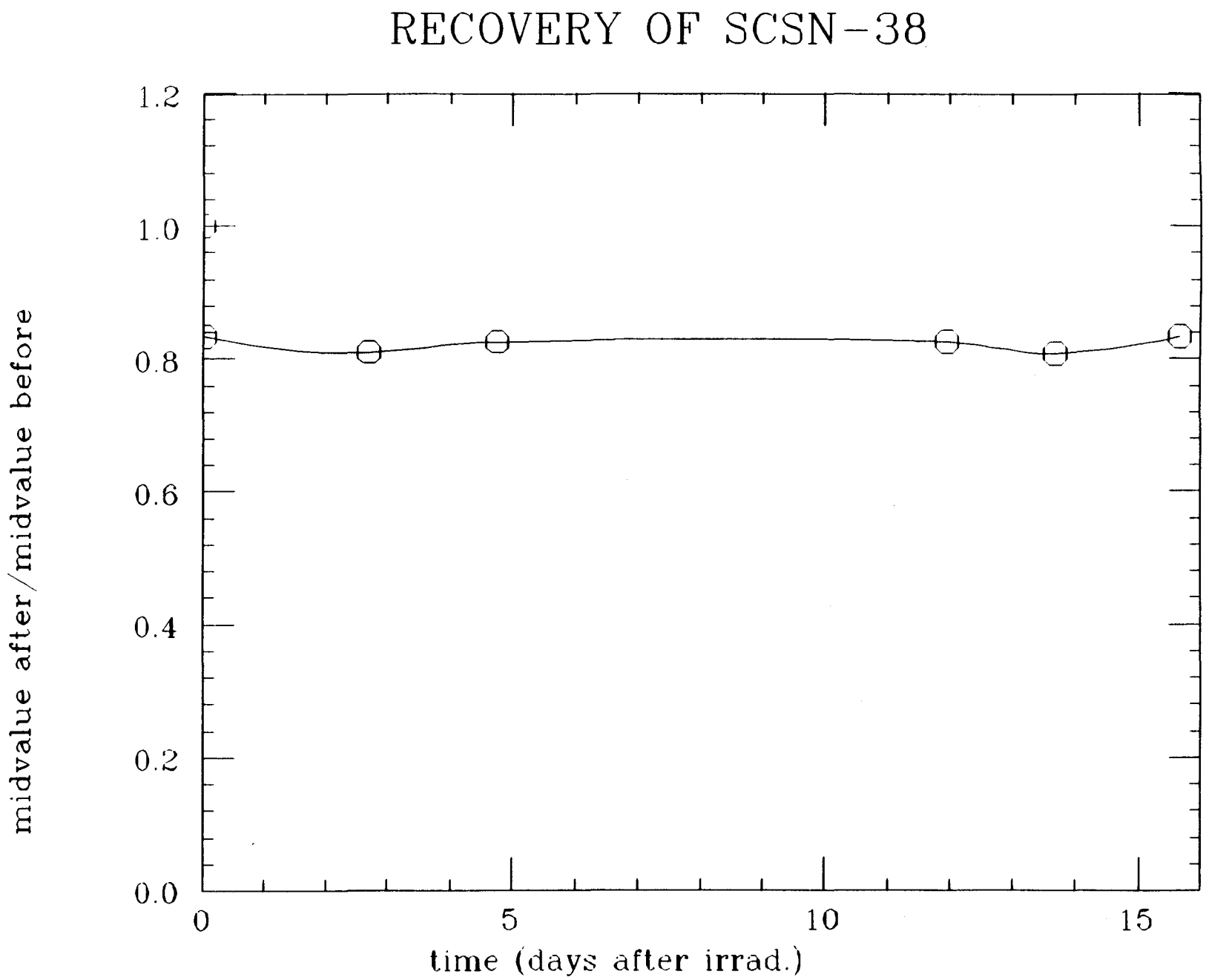
RECOVERY OF SCSN-38
1.2
1.0
0.8
0.6
0.4
0.2
0.0
0
5
10
15
midvalue after/midvalue before
time (days after irrad.)

FIG. 16

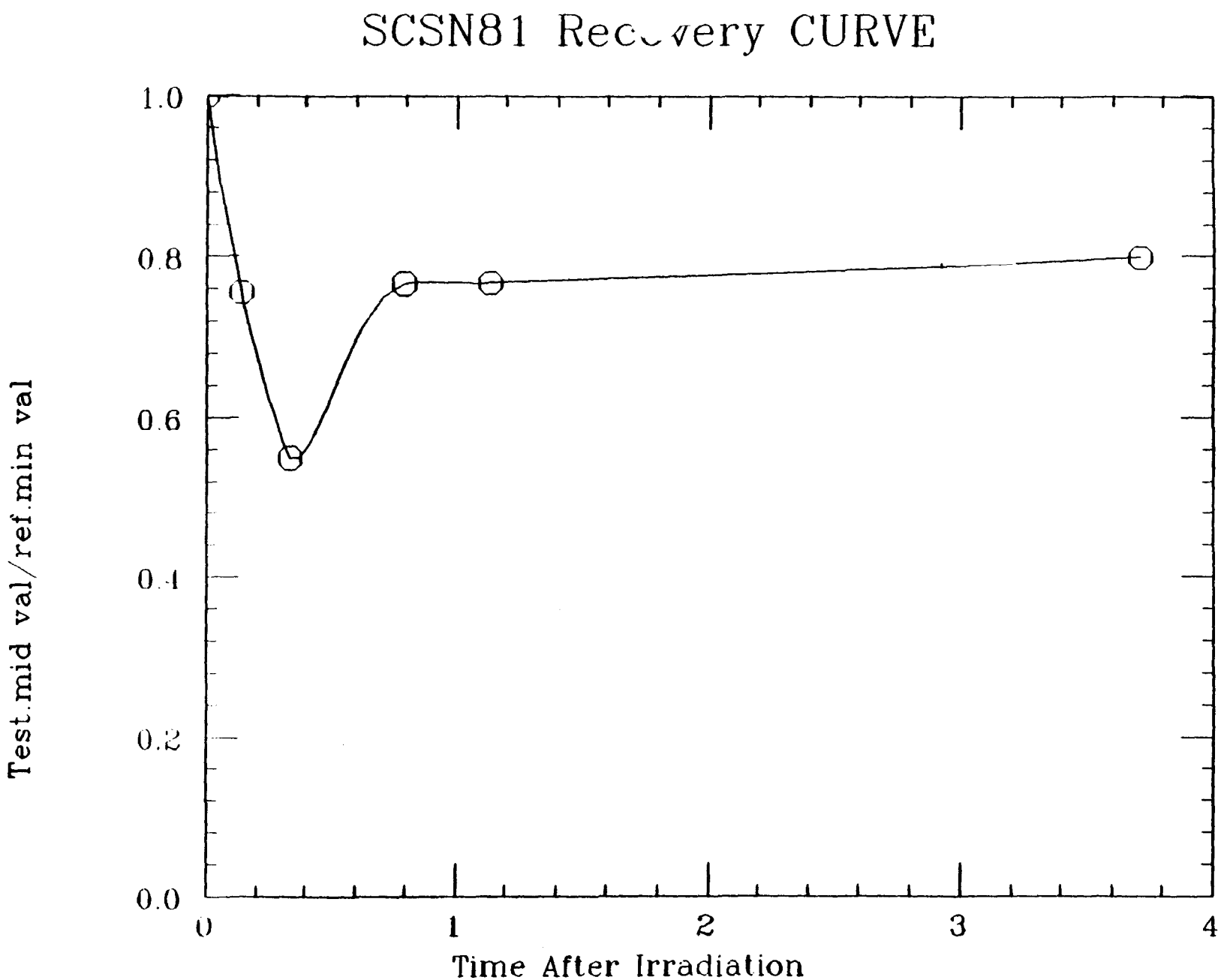
SCSN81 Recovery CURVE
1.0
0.8
0.6
0.4
0.2
0.0
Test.mid val/ref.min val
0
1
2
3
4
Time After Irradiation

FIG. 17

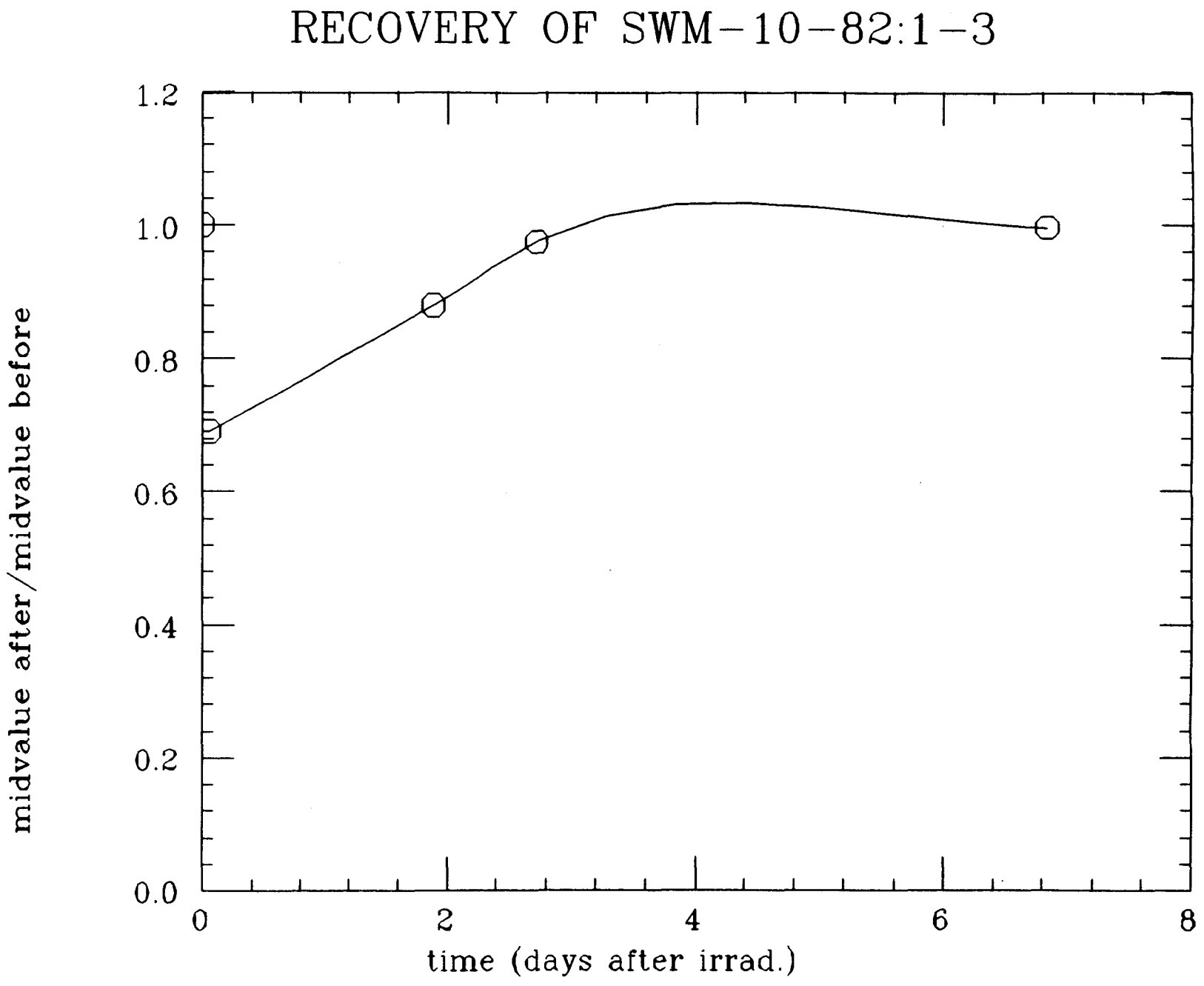
RECOVERY OF SWM-10-82:1-3
1.2
1.0
0.8
0.6
0.4
0.2
0.0
0
2
4
6
8
midvalue after/midvalue before
time (days after irrad.)

FIG. 18

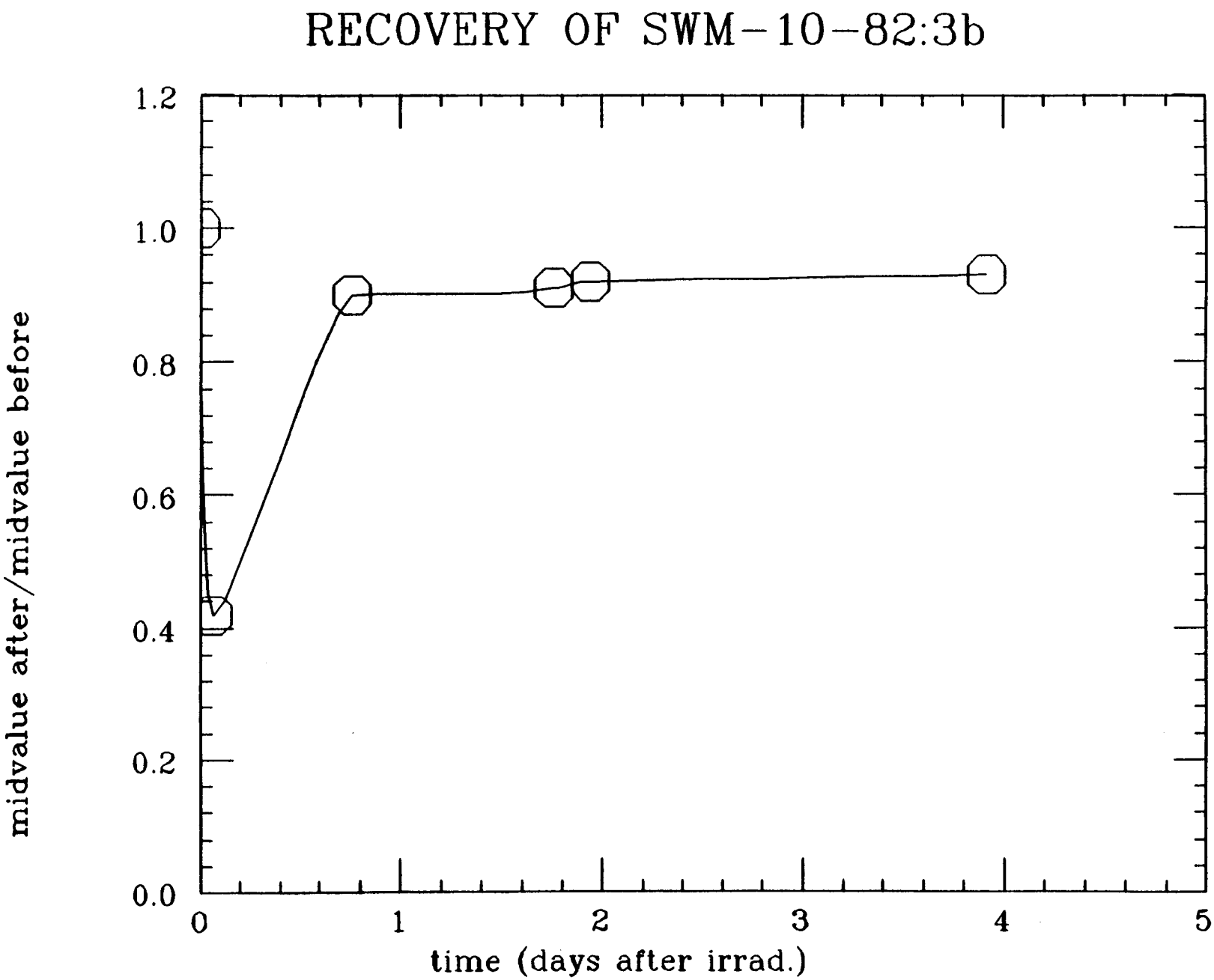
RECOVERY OF SWM-10-82:3b
1.2
1.0
0.8
0.6
0.4
0.2
0.0
0
1
2
3
4
5
midvalue after/midvalue before
time (days after irrad.)

FIG. 19

RH-4 ATTENUATION CURVES

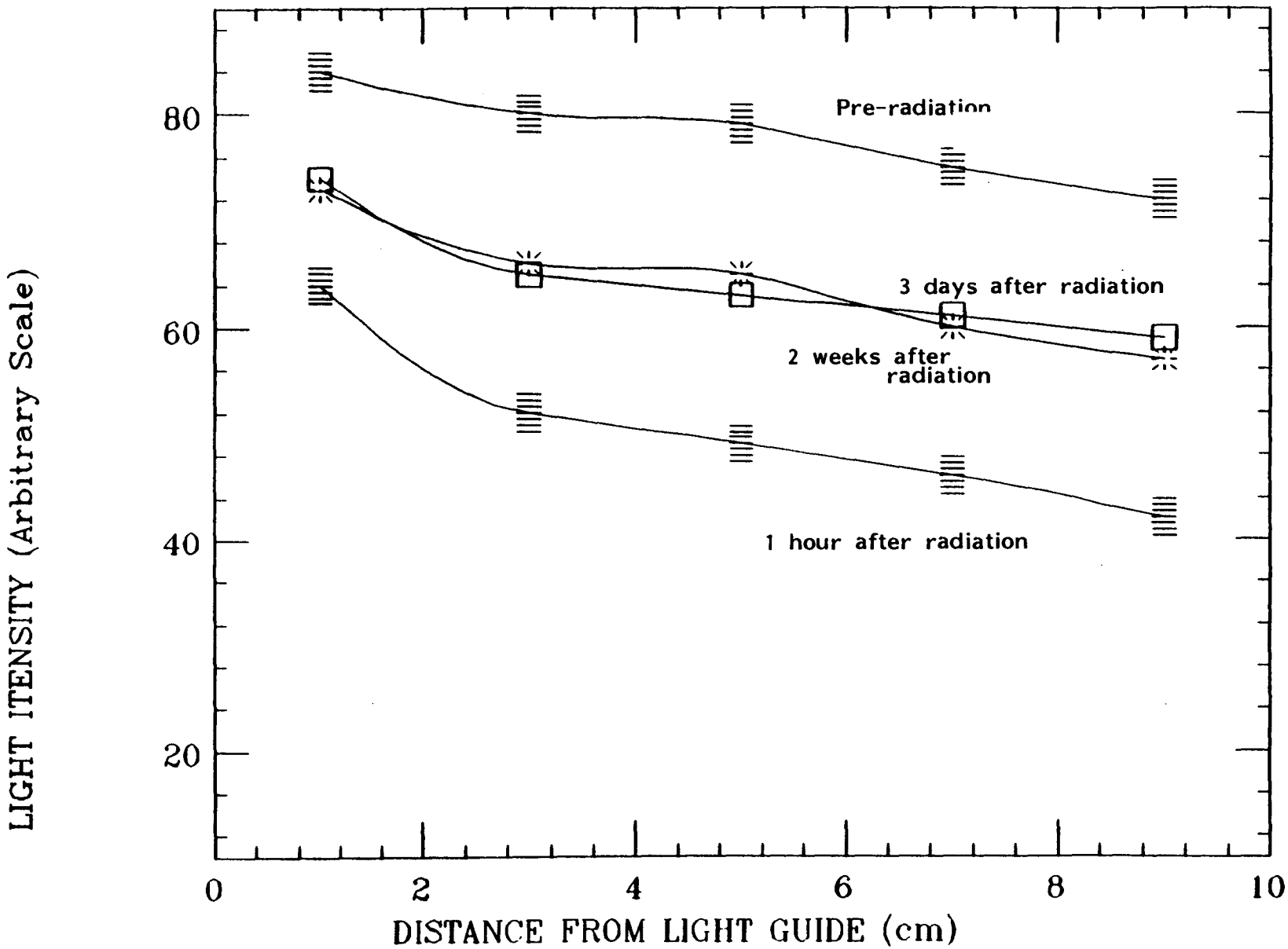

FIG. 20

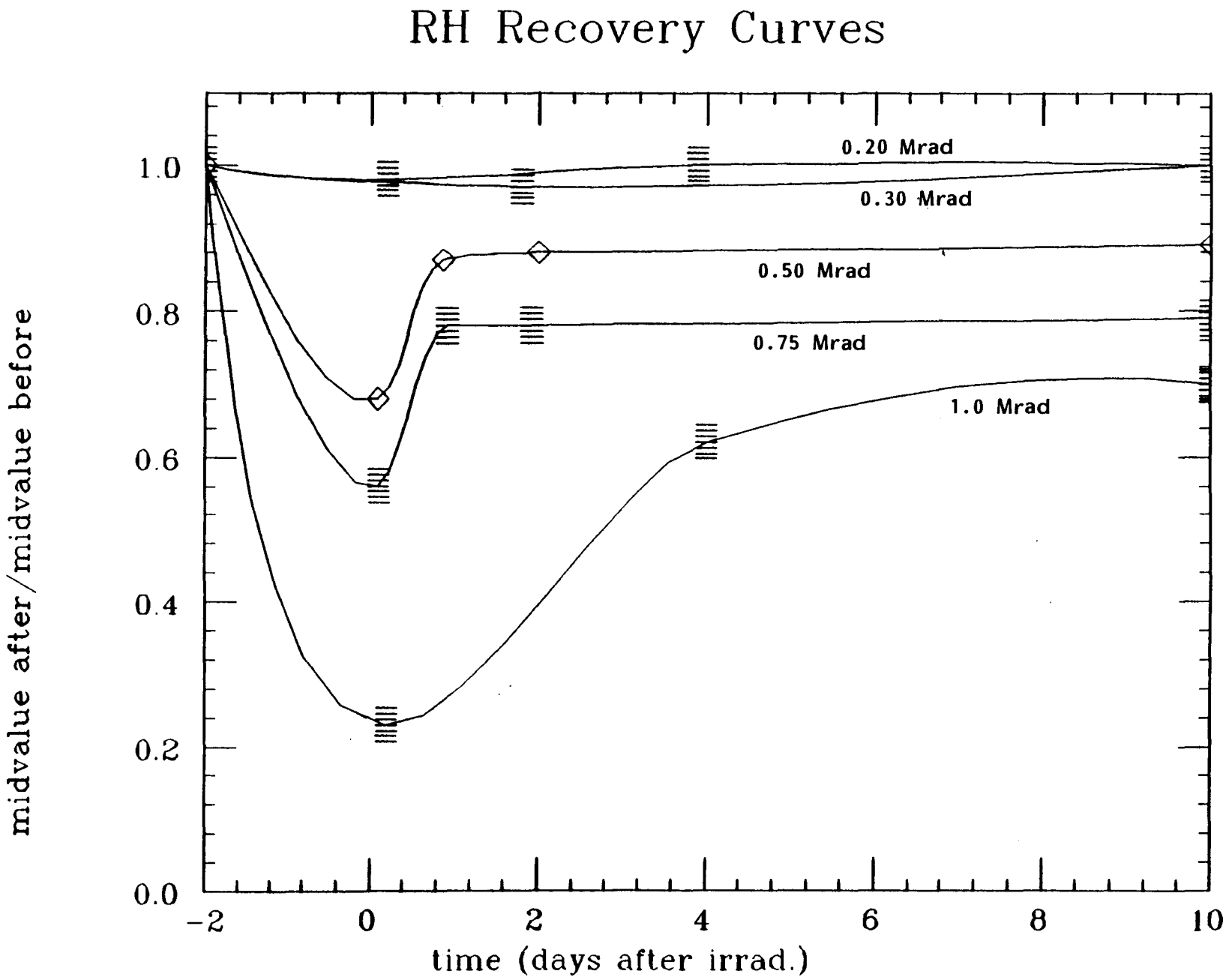
RH Recovery Curves
0.20 Mrad
0.30 Mrad
0.50 Mrad
0.75 Mrad
1.0 Mrad
1.0
0.8
0.6
0.4
0.2
0.0
-2
0
2
4
6
8
10
midvalue after/midvalue before
time (days after irrad.)

FIG. 21

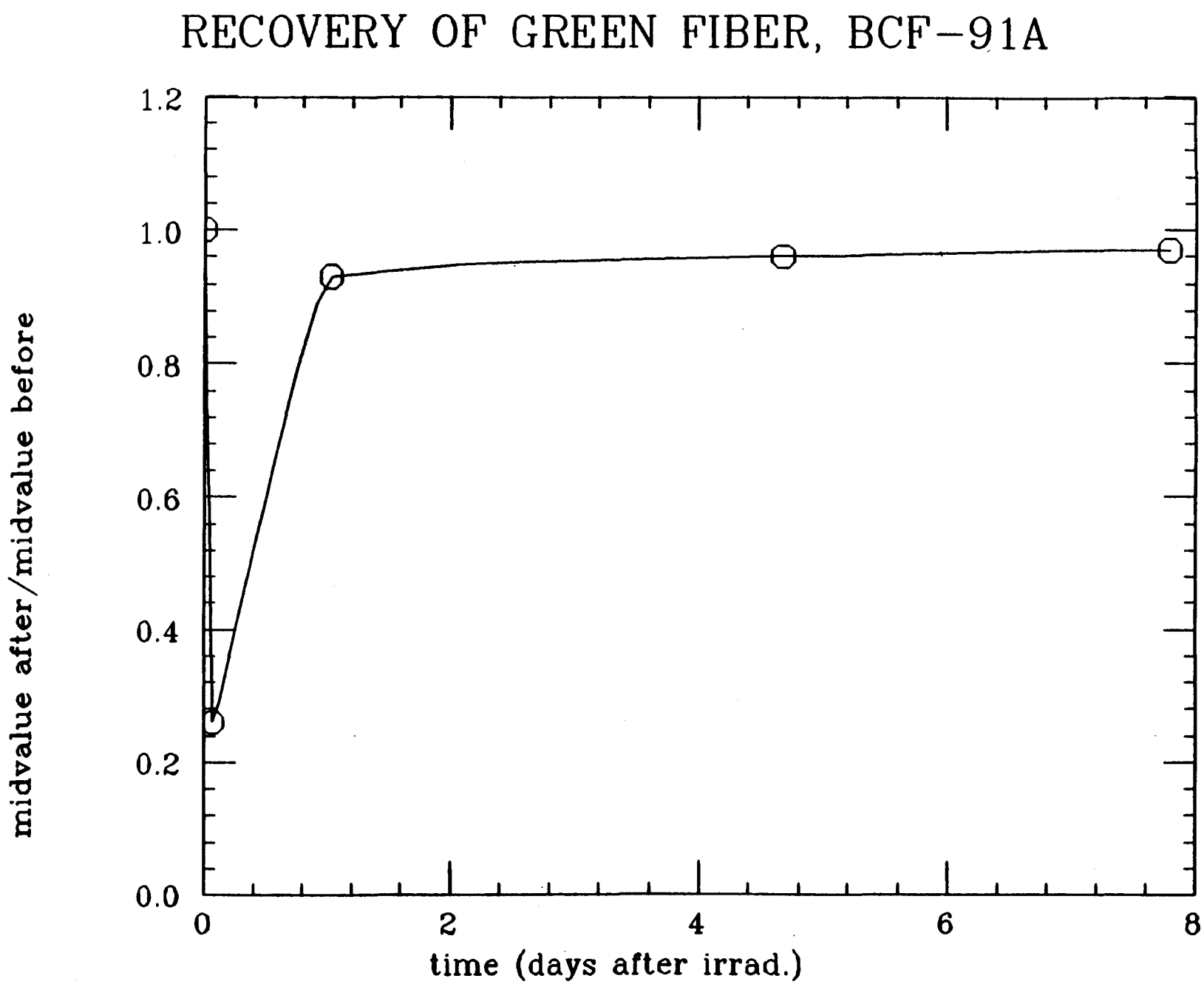
RECOVERY OF GREEN FIBER, BCF-91A
1.2
1.0
0.8
0.6
0.4
0.2
0.0
0
2
4
6
8
midvalue after/midvalue before
time (days after irrad.)

FIG. 22